International Journal of Web of Multidisciplinary Studies
(Peer-Reviewed, Open Access, Fully Refereed International Journal)
website: https://ijwos.com OPEN ACCESS E-ISSN : 3049-2424
Volume 3 Issue 8 , August 2026 DOI: https://doi.org/10.71366/ijwos03082636502

In Silico Screening of Potential Phytochemical Inhibitors against Human Hematopoietic Prostaglandin D2 Synthase (hH-PGDS) for Anti-Allergic and Anti-Inflammatory Drug Development

Astha Jaiswal[1], Vinay Kumar Singh[2]
[1] *Department of Biotechnology, Ashoka Institute of Technology and Management, Varanasi, Uttar Pradesh 221007;*
[2] *Centre for Bioinformatics, School of Biotechnology, Institute of Science, Banaras Hindu University, Varanasi, Uttar Pradesh 221005.*

Article Info

Article History:

Published: 16 August 2026

Publication Issue:
Volume 3, Issue 8
August-2026

Page Number:
306-330

Corresponding Author:
Vinay Kumar Singh

Abstract:

Human hematopoietic prostaglandin D2 synthase (hH-PGDS) is a key enzyme responsible for the biosynthesis of prostaglandin D2 (PGD2), an important lipid mediator involved in allergic responses, inflammation, asthma, and immune regulation. Inhibition of hH-PGDS represents a promising therapeutic strategy for developing novel anti-allergic and anti-inflammatory agents. The present study aimed to identify potential phytochemical inhibitors targeting hH-PGDS using structure-based virtual screening and molecular docking approaches.

A total of 890 phytochemical compounds were retrieved from the PubChem database and screened against the active site of hH-PGDS (UNIPROT ID: O60760; PDB ID: 5AIV) using LibDock protocol implemented in BIOVIA Discovery Studio 2019. The experimentally reported indole inhibitor of hH-PGDS was selected as the reference compound, exhibiting a LibDock score of 123.347 and CDOCKER interaction energy of 30.0771. Based on LibDock ranking, 39 phytochemicals were selected for further evaluation. The top five candidates were subsequently analyzed using the CDOCKER docking algorithm to evaluate binding affinity, interaction pattern, and molecular stability within the enzyme active site.

The potential identified 2 phytochemicals (Salvianolic acid A Compound CID: 5281793 & Calceolarioside B Compound CID: 5273567) demonstrated favorable binding interactions with important catalytic and active-site residues of hH-PGDS, suggesting their potential inhibitory activity. The screened compounds may serve as promising lead molecules for further experimental validation and development of novel anti-inflammatory and anti-allergic therapeutics.

Keywords: hH-PGDS; prostaglandin D2 synthase; phytochemicals; molecular docking; LibDock; CDOCKER; anti-inflammatory; anti-allergic agents; virtual screening

1. Introduction

Inflammatory disorders and allergic diseases represent major global health concerns due to their increasing prevalence and impact on quality of life. The inflammatory response is regulated by various signaling molecules, among which prostaglandins play essential roles in immune modulation and pathological inflammation (Catalan-Serra & Sebastian, 2025; Alska et al., 2025; Carron et al., 2010; Luo et al., 2024).

Prostaglandin D2 (PGD2) is a major inflammatory mediator generated through the conversion of prostaglandin H2 (PGH2). In humans, PGD2 production is primarily regulated by two prostaglandin D2 synthase enzymes: lipocalin-type prostaglandin D2 synthase and hematopoietic prostaglandin D2 synthase (hH-PGDS) (Li et al., 2025). hH-PGDS is highly expressed in mast cells and contributes significantly to allergic inflammation by promoting activation of immune cells through PGD2-mediated pathways.

Inhibition of hH-PGDS has emerged as a potential strategy for controlling allergic and inflammatory diseases including asthma, dermatitis, and other immune-related disorders. Several synthetic inhibitors have been developed; however, identification of safe and effective molecules remains an important research objective.

Natural phytochemicals represent a valuable source of bioactive compounds with diverse pharmacological properties, including antioxidant, anti-inflammatory, and Erectile Dysfunction. Computational approaches such as molecular docking and virtual screening provide efficient methods for identifying potential enzyme inhibitors from large chemical libraries (Boudou et al., 2026).

In the present study, a structure-based virtual screening approach was applied to identify potential phytochemical inhibitors against hH-PGDS. The crystal structure of hH-PGDS complexed with an active-site inhibitor (PDB ID: 5AIV) was used as the target protein. The reported indole inhibitor identified by Fredrik Edfeldt and colleagues was selected as a reference molecule for validating docking performance (Edfeldt et al. 2015).

2. Materials and Methods

2.1 Target Protein Preparation

The three-dimensional crystal structure of human hematopoietic prostaglandin D2 synthase (hH-PGDS) complexed with an active-site inhibitor was obtained from the Protein Data Bank with accession number 5AIV (Burley et al., 2017). Protein preparation was performed using BIOVIA Discovery Studio 2019 (https://www.3ds.com/products/biovia/discovery-studio). Water molecules, unwanted heteroatoms, and crystallographic contaminants were removed. Missing hydrogen atoms were added, and the protein structure was optimized prior to docking analysis.

2.2 Selection of Reference Inhibitor

The reported indole-based inhibitor of hH-PGDS described by Edfeldt et al. (2015) was selected as the standard inhibitor for comparative analysis. The reference compound was docked into the active site of hH-PGDS, and docking parameters were used as validation criteria.

2.3 Phytochemical Dataset Preparation

A total of 890 phytochemical compounds were retrieved from the PubChem database and subjected to ligand preparation using BIOVIA Discovery Studio 2019 (Kim et al., 2016). The collected compounds were processed to ensure structural accuracy and suitability for molecular docking analysis. During the preparation process, duplicate structures were removed to eliminate redundancy, followed by the generation of three-dimensional conformations of the ligands. Energy minimization was performed to optimize the molecular geometries and obtain energetically stable conformations. The prepared ligand library was subsequently used for virtual screening and docking studies against the active site of human hematopoietic prostaglandin D2 synthase (hH-PGDS).

2.4 Virtual Screening Using LibDock

Initial screening of phytochemical compounds was performed using the LibDock protocol. The active site of hH-PGDS was defined based on the co-crystallized inhibitor binding region. The prepared phytochemicals were docked into the active site, and compounds were ranked according to LibDock score. Superior docking scores compared with the reference inhibitor were selected for further analysis (Diller & Merz, 2001).

2.5 Molecular Docking Using CDOCKER

The top-ranked 39 compounds obtained from the LibDock screening were further subjected to CDOCKER analysis using BIOVIA Discovery Studio 2019. CDOCKER is a CHARMm-based molecular dynamics docking algorithm used to evaluate ligand-protein interactions and predict binding affinity within the active site of hH-PGDS (Wu et al.,

2003). The analysis provided important docking parameters, including CDOCKER interaction energy, CDOCKER energy, hydrogen bonding interactions, hydrophobic interactions, and binding pose characteristics. The binding orientations and interaction profiles of the screened compounds were compared with the reference inhibitor to identify molecules exhibiting favorable interactions with the target protein. Based on their docking scores, interaction energies, and stable binding patterns, the five compounds with the most promising docking properties were selected as potential inhibitors of human hematopoietic prostaglandin D2 synthase (hH-PGDS).

2.6 Simulation Protocol & Trajectory Analysis

The three-dimensional crystal structure of the core protein (PDB ID: 5AIV) was retrieved from the Protein Data Bank (PDB). Screened bioactive compounds were selected for dynamics studies. The apo-protein system (5AIV) was prepared without any ligand and the screened complex systems were used for standard dynamics cascade analysis. All systems were explicitly solvated using a water model to mimic physiological conditions. Molecular dynamics (MD) simulations were conducted using the Standard Dynamics Cascade (SDC) protocol within BIOVIA Discovery Studio 2019. The SDC simulations were performed with the default parameters as provided by the software, without any manual modifications to the integration steps, temperature coupling, or pressure control algorithms. Prior to the production runs, energy minimization was carried out to remove any steric clashes and to relax the solvated systems.

Post-simulation, the trajectories were analyzed to evaluate the structural stability and dynamic behavior of the three systems. Root Mean Square Deviation (RMSD) was calculated for the Cα atoms of the protein backbone to measure the conformational drift of each system relative to its initial minimized structure over the simulation timeframe. Root Mean Square Fluctuation (RMSF) was computed per residue to assess the local flexibility and mobility of individual amino acids throughout the simulation. All trajectory analyses, including RMSD and RMSF calculations, were performed using the built-in analysis modules of Discovery Studio 2019. Validation of the simulation parameters and system equilibration was verified through the generated validation slider images.

3. Results

The 3D structure of human hematopoietic prostagandin D2 synthase (hH-PGDS) in complex with an active site inhibitor M1W (3-(1H-indol-4-yl)-N-(3-methoxypropyl)-1,2,4-oxadiazole-5-carboxamide) in PDB format (**Figure 1**).

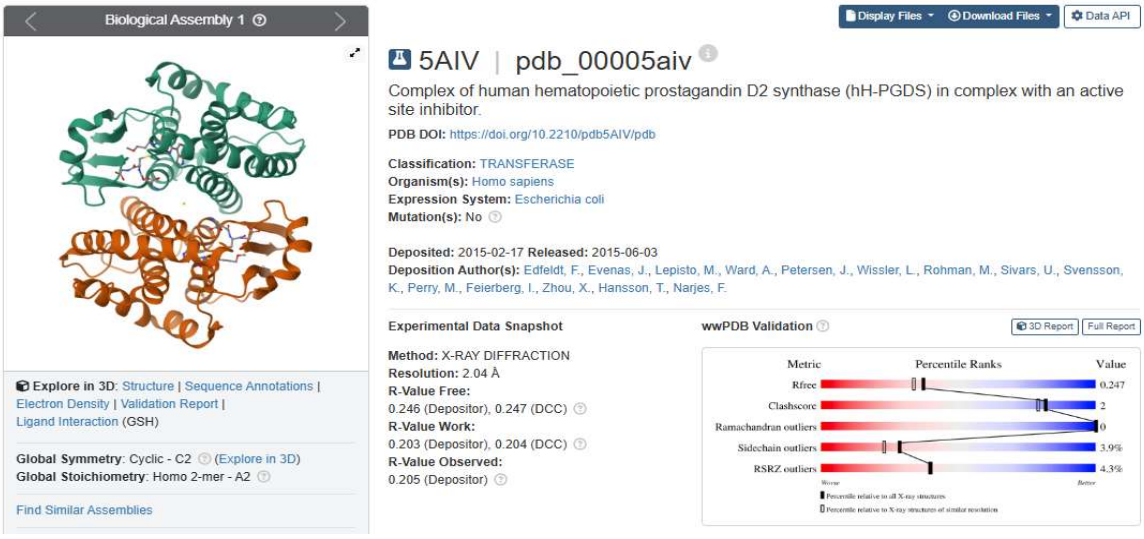

Figure 1: PDB file details (wwPDB validation) for hH-PGDS

3.1 Virtual Screening of Phytochemicals

The LibDock Score for control inhibitor M1W (3-(1H-indol-4-yl)-N-(3-methoxypropyl)-1,2,4-oxadiazole-5-carboxamide) was generated using docking calculation (**Figure 2**).

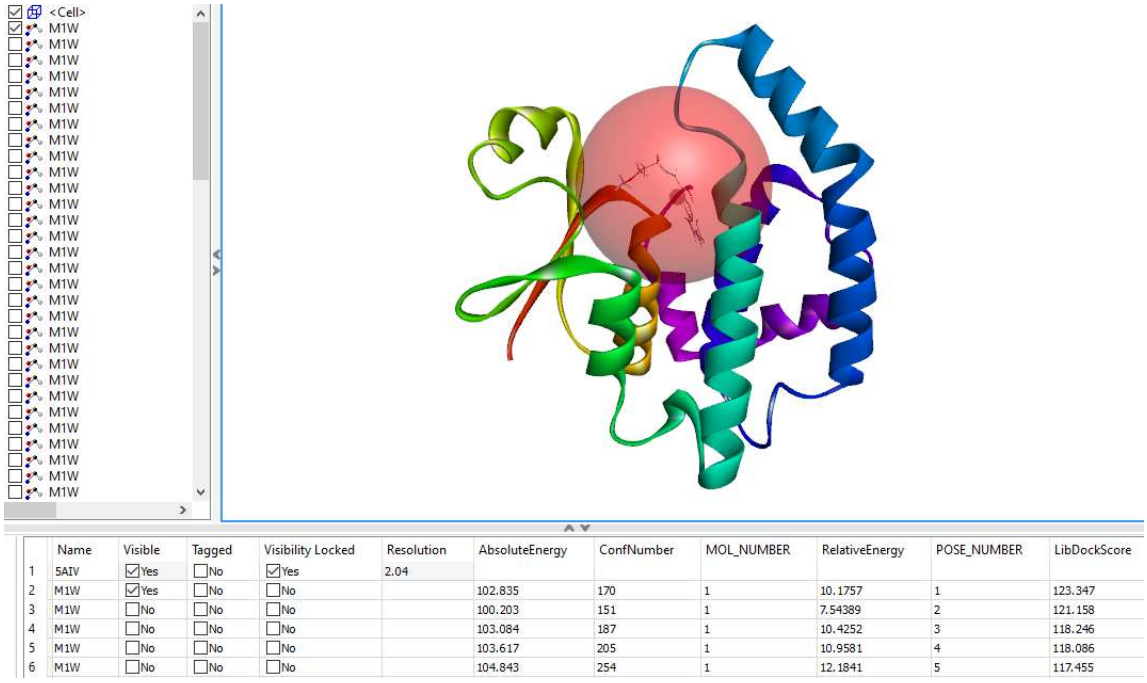

Figure 2: LibDock Score for Control Compound M1W (CID: 42571591; 3-(1H-indol-4-yl)-N-(3-methoxypropyl)-1,2,4-oxadiazole-5-carboxamide) complex with hH-PGDS

The virtual screening process identified 39 phytochemicals compounds showing strong interaction potential against the active site of hH-PGDS (**Table 1**). Compared with the reference inhibitor LibDock score 123.347, selected compounds demonstrated comparable or improved docking scores, indicating their potential ability to bind within the catalytic pocket.

Table 1. Selected phytochemicals based on LibDock screening

Compound_CID	Name	Molecular_Weight	Molecular_Formula	XLogP	Heavy_Atom_Count	H-Bond_Donor_Count	H-Bond_Acceptor_Count
10621	Hesperidin	610.6	C28H34O15	-1.1	43	8	15
30231	Neohesperidin dihydrochalcone	612.6	C28H36O15	-0.3	43	9	15
64982	Baicalin	446.4	C21H18O11	1.1	32	6	11
83489	Eriocitrin	596.5	C27H32O15	-1.4	42	9	15
146798	Procyanidin B3	578.5	C30H26O12	2.4	42	10	12

168849	Pectolinarin	622.6	C29H34O15	-0.5	44	7	15
185617	Scutellarin	462.4	C21H18O12	0.8	33	7	12
442416	Agnuside	466.4	C22H26O11	-1.1	33	6	11
442431	Narirutin	580.5	C27H32O14	-1.1	41	8	14
442439	Neohesperidin	610.6	C28H34O15	-0.5	43	8	15
452707	1,3,6-Tri-O-Galloyl-Beta-D-Glucose	636.5	C27H24O18	0.4	45	11	18
5273567	Calceolarioside B	478.4	C23H26O11	0.6	34	7	11
5280746	Apiin	564.5	C26H28O14	-0.4	40	8	14
5281613	Diosmin	608.5	C28H32O15	-0.8	43	8	15
5281773	Forsythoside A	624.6	C29H36O15	-0.5	44	9	15
5281788	Plantamajoside	640.6	C29H36O16	-1	45	10	16
5281793	Salvianolic acid	494.4	C26H22O10	3.9	36	7	10
5281800	Verbascoside	624.6	C29H36O15	-0.5	44	9	15
5282150	Rhoifolin	578.5	C27H30O14	-0.2	41	8	14
5284419	Methylhesperidin	624.6	C29H36O15	-0.8	44	7	15
5317025	Linarin	592.5	C28H32O14	-0.5	42	7	14
5319484	Apigenin 7-O-glucuronide	446.4	C21H18O11	0.2	32	6	11
6440783	3,4,5-Tricaffeoylquinic acid	678.6	C34H30O15	3.5	49	8	15
6441498	Lithospermic Acid	538.5	C27H22O12	2.8	39	7	12
6442433	Isoliquiritin Apioside	550.5	C26H30O13	0.1	39	8	13
6443484	Mulberroside A	568.5	C26H32O14	-0.8	40	10	14
6476333	Isoacteoside	624.6	C29H36O15	-0.5	44	9	15
6918448	Neomangiferin	584.5	C25H28O16	-2.2	41	11	16

9917980	Secoisolariciresinol Diglucoside	686.7	C32H46O16	-0.7	48	10	16
10076238	Liquiritin apioside	550.5	C26H30O13	-0.8	39	7	13
10077207	Baicalein 7-O-diglucoside	594.5	C27H30O15	-1.3	42	9	15
11016019	Diosmetin 7-O-beta-D-glucoside	462.4	C22H22O11	0.8	33	6	11
13991590	Salvianolic acid C	492.4	C26H20O10	4.1	36	6	10
14034912	Prim-O-Glucosylcimifugin	468.4	C22H28O11	-0.9	33	5	11
21629996	2-Acetylacteoside	666.6	C31H38O16	0.1	47	8	16
24121289	6-O-trans-Feruloylcatalpol	538.5	C25H30O13	-0.9	38	6	13
59054533	1,3,5-tris[[(E)-3-(3,4-dihydroxyphenyl)prop-2-enoyl]oxy]-4-hydroxycyclohexane-1-carboxylic acid	678.6	C34H30O15	3.5	49	8	15
71522062	(2R,3R,4S,5R,6R)-2-(3,4-Dihydroxyphenethoxy)-3,5-dihydroxy-6-((((2S,3R,4R,5R,6S)-3,4,5-trihydroxy-6-methyltetrahydro-2H-pyran-2-yl)oxy)methyl)tetrahydro-2H-pyran-4-yl (E)-3-(3,4-dihydroxyphenyl) acrylate	624.6	C29H36O15	-0.5	44	9	15
102594479	2-O-beta-L-galactopyranosylorientin	610.5	C27H30O16	-1.7	43	11	16

3.2 CDOCKER Analysis of Candidate Compounds

The screened 39 phytochemicals compounds were used for CDOCKER based docking and compared control M1W (CID: 42571591; **Figure 3**).

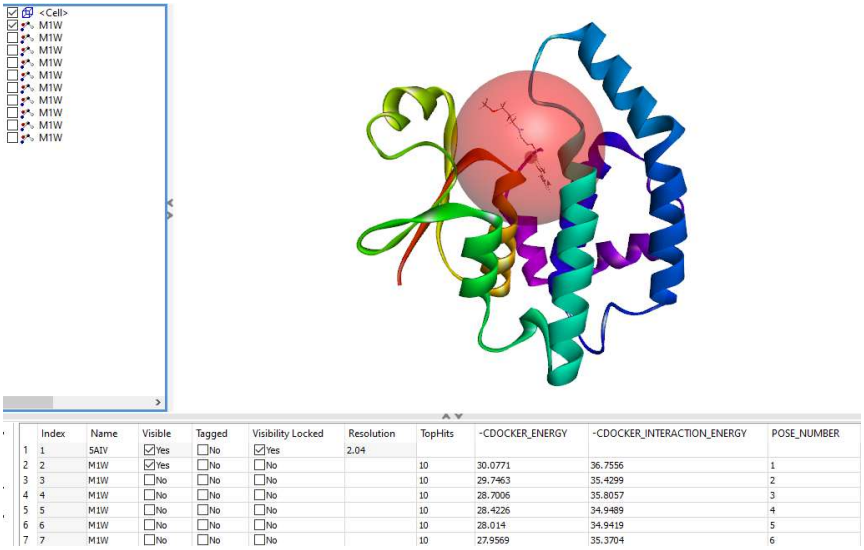

	Index	Name	Visible	Tagged	Visibility Locked	Resolution	TopHits	-CDOCKER_ENERGY	-CDOCKER_INTERACTION_ENERGY	POSE_NUMBER
1	1	SAIV	Yes	No	Yes	2.04				
2	2	M1W	Yes	No	No		10	30.0771	36.7556	1
3	3	M1W	No	No	No		10	29.7463	35.4299	2
4	4	M1W	No	No	No		10	28.7006	35.8057	3
5	5	M1W	No	No	No		10	28.4226	34.9489	4
6	6	M1W	No	No	No		10	28.014	34.9419	5
7	7	M1W	No	No	No		10	27.9569	35.3704	6

Figure 3: -CDCKER ENERGY Score for Control Compound M1W (CID: 42571591; 3-(1H-indol-4-yl)-N-(3-methoxypropyl)-1,2,4-oxadiazole-5-carboxamide) complex with hH-PGDS

The five selected phytochemicals were further evaluated using control CDOCKER energy 30.0771 (**Table 2**; **Table 3**). The docking analysis revealed strong binding interactions with important residues located in the hH-PGDS active site of control complex (**Figure 4**). Based on analysis only 2 most prominent compounds (CID 5273567 & CID 5281793) were selected finally (**Table 3**; **Figure 5-6**).

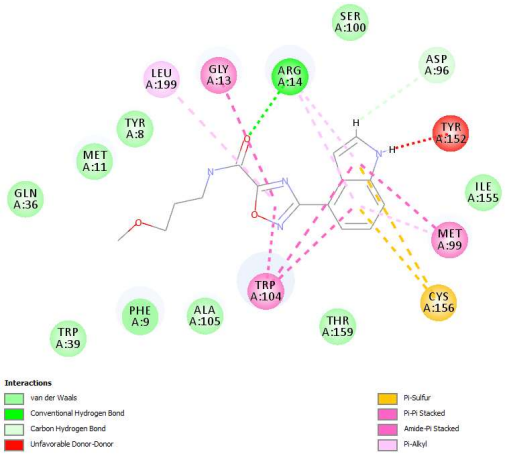

Figure 4: 2D interaction details of Control Compound M1W (CID: 42571591)

Table 2: CDOCKER MD based docking of 39 screened compounds

Name	Visible	Tagged	Visibility Locked	Resolution	TopHits	-CDOCKER_ENERGY	-CDOCKER_INTERACTION_ENERGY	POSE_NUMBER
452707	No	No	No		10	60.4178	58.8559	8
452707	No	No	No		10	60.1412	67.1866	9
452707	No	No	No		10	60.1044	57.509	10
5281793	No	No	No		10	51.9997	57.1775	1
5281793	No	No	No		10	47.3707	53.3482	2
5281793	No	No	No		10	46.4101	50.3622	3
13991590	No	No	No		10	46.1039	59.2379	1
5281793	No	No	No		10	45.1847	55.332	4
13991590	No	No	No		10	43.4052	54.6355	2
5281793	No	No	No		10	43.296	55.2189	5
5281793	No	No	No		10	43.2261	52.8663	6
5281793	No	No	No		10	42.7375	57.2239	7
5281793	No	No	No		10	42.0485	51.2713	8
5281793	No	No	No		10	41.9162	54.0724	9
13991590	No	No	No		10	41.2365	52.8475	3
13991590	No	No	No		10	40.3989	48.6907	4
6441498	No	No	No		10	40.0913	58.6563	1
5281793	No	No	No		10	39.8717	46.0379	10
13991590	No	No	No		10	39.7755	55.003	5
13991590	No	No	No		10	39.1092	43.6328	6
13991590	No	No	No		10	38.9844	57.8481	7
13991590	No	No	No		10	38.8333	45.2386	8
6441498	No	No	No		10	38.7135	56.3303	2
13991590	No	No	No		10	38.63	43.2664	9
13991590	No	No	No		10	37.7352	53.1405	10
6441498	No	No	No		10	35.8069	60.1484	3
6441498	No	No	No		10	35.2221	62.274	4
6441498	No	No	No		10	34.7975	58.301	5
6441498	No	No	No		10	34.3258	57.8764	6
6441498	No	No	No		10	34.1656	52.8028	7
6441498	No	No	No		10	34.1168	53.4289	8
6441498	No	No	No		10	33.4718	58.1383	9
6441498	No	No	No		10	32.4811	55.9054	10
5273567	No	No	No		10	31.02	55.1704	1

Table 3. CDOCKER docking results

Compound_CID	Name	Molecular_Weight	Molecular_Formula	Polar_Area	Complexity	XLogP	Heavy_Atom_Count	H-Bond_Donor_Count	H-Bond_Acceptor_Count
452707	1,3,6-Tri-O-Galloyl-Beta-D-Glucose	636.5	C27H24O18	311	1010	0.4	45	11	18
5273567	Calceolarioside B	478.4	C23H26O11	186	673	0.6	34	7	11
5281793	Salvianolic acid	494.4	C26H22O10	185	798	3.9	36	7	10
6441498	Lithospermic Acid	538.5	C27H22O12	211	922	2.8	39	7	12

13991590	Salvianolic acid C	492.4	C26H20O10	178	802	4.1	36	6	10

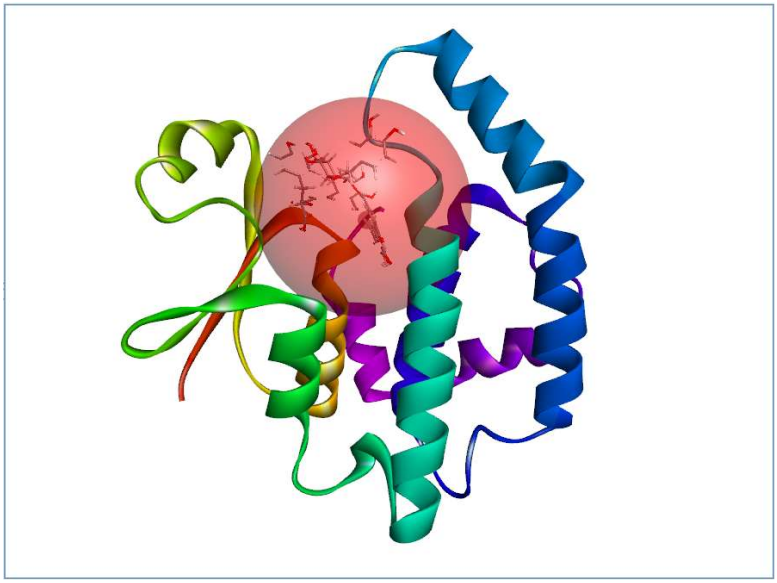

Figure 5: 3D representation of 2 most prominent compounds (CID 5273567 & CID 5281793)

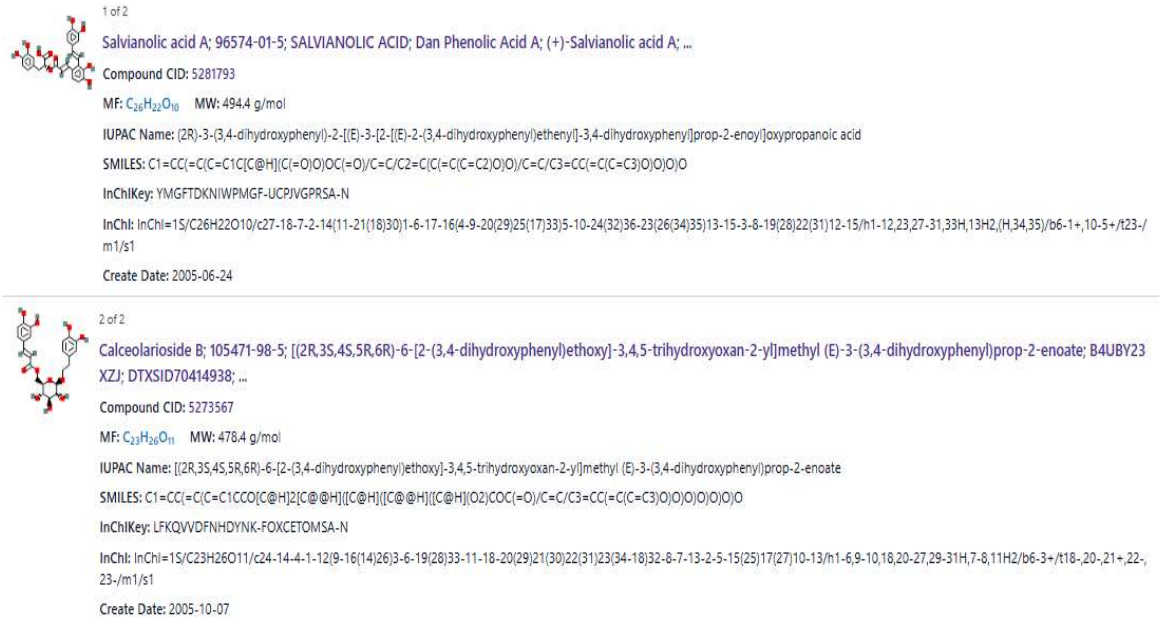

Figure 6: Details of 2 best identified compounds (CID 5273567 & CID 5281793)

Comparative analysis of binding energy (kcal/mol) between control and screened was performed all 5 screened compound showed better binding energy in comparison to control (**Table 4** & **Table 5**).

Table 4. Binding Energy of control

Ligand Name	Binding Energy (kcal/mol)	Ligand Energy (kcal/mol)	Protein Energy (kcal/mol)	Complex Energy (kcal/mol)	Entropic Energy (kcal/mol)
M1W	-42.5810	7.9702	-6483.8584	-6518.4691	19.5631
M1W	-53.3263	5.4878	-6483.8584	-6531.6969	19.6072
M1W	-63.8531	9.2380	-6483.8584	-6538.4735	19.5697
M1W	-26.0789	7.3231	-6483.8584	-6502.6142	19.4852
M1W	-33.0850	6.2297	-6483.8584	-6510.7137	19.5600
M1W	-46.3094	6.4888	-6483.8584	-6523.6789	19.5272
M1W	-28.0965	7.0141	-6483.8584	-6504.9408	19.5556
M1W	-34.2855	5.3231	-6483.8584	-6512.8207	19.5916
M1W	-62.1540	5.5733	-6483.8584	-6540.4391	19.6011
M1W	-38.6869	9.3875	-6483.8584	-6513.1578	19.5193

Table 5. Binding Energy of screened molecules

Ligand Name	Binding Energy (kcal/mol)	Ligand Energy (kcal/mol)	Protein Energy (kcal/mol)	Complex Energy (kcal/mol)	Entropic Energy (kcal/mol)
452707	-101.7219	-125.8700	-6483.8584	-6711.4502	21.6981
452707	-80.7840	-126.8401	-6483.8584	-6691.4824	21.6969
452707	-68.9830	-125.3434	-6483.8584	-6678.1847	21.6911
452707	-86.3802	-136.8809	-6483.8584	-6707.1194	21.4661
452707	-140.9464	-115.1479	-6483.8584	-6739.9527	21.6101
452707	-43.8906	-170.7471	-6483.8584	-6698.4960	21.6238
452707	-90.4511	-134.5438	-6483.8584	-6708.8532	21.6769
452707	-122.5349	-149.3687	-6483.8584	-6755.7619	21.5470
452707	-115.1497	-146.5203	-6483.8584	-6745.5283	21.6162
452707	-134.1005	-155.1756	-6483.8584	-6773.1344	21.5700
5273567	-124.3695	-17.9251	-6483.8584	-6626.1529	20.8705
5281793	-120.5044	-54.4984	-6483.8584	-6658.8611	20.8552
5281793	-73.0206	-59.5259	-6483.8584	-6616.4048	20.9514
5281793	-105.9730	-58.5597	-6483.8584	-6648.3910	20.9727
5281793	-7.9413	-43.3843	-6483.8584	-6535.1839	21.0722
5281793	-140.6070	-45.8740	-6483.8584	-6670.3394	20.9132
5281793	10.8868	-50.1189	-6483.8584	-6523.0904	20.9365
5281793	-103.9043	-42.2467	-6483.8584	-6630.0094	20.9087
5281793	-12.1346	-54.4559	-6483.8584	-6550.4488	20.9341
5281793	-6.5712	-53.3578	-6483.8584	-6543.7873	20.9831
5281793	-57.4503	-57.9136	-6483.8584	-6599.2223	20.9647
6441498	-52.6593	-61.9030	-6483.8584	-6598.4207	21.1688
6441498	-46.3586	-51.3265	-6483.8584	-6581.5434	21.1876
6441498	-86.1626	-46.7625	-6483.8584	-6616.7834	21.1112
6441498	-104.3031	-38.2807	-6483.8584	-6626.4421	21.1034
6441498	-34.2038	-36.4162	-6483.8584	-6554.4784	21.1016
6441498	-143.1081	-52.5627	-6483.8584	-6679.5292	21.0977
6441498	-52.7097	-61.0234	-6483.8584	-6597.5915	21.1437
6441498	-68.3089	-62.6404	-6483.8584	-6614.8077	21.1464
6441498	-59.4166	-41.9218	-6483.8584	-6585.1967	21.1320
6441498	-17.9033	-55.6110	-6483.8584	-6557.3726	21.0397
13991590	-84.9206	-40.9258	-6483.8584	-6609.7048	21.0585
13991590	-45.8923	-45.6224	-6483.8584	-6575.3731	21.0595
13991590	-85.6502	-48.0129	-6483.8584	-6617.5215	21.0434
13991590	-33.4540	-57.7906	-6483.8584	-6575.1029	20.9058
13991590	-64.4273	-39.0240	-6483.8584	-6587.3097	21.1093
13991590	-77.2671	-48.7665	-6483.8584	-6609.8919	20.7904
13991590	-101.1964	-31.1866	-6483.8584	-6616.2414	21.0155
13991590	-28.8166	-62.9647	-6483.8584	-6575.6397	20.8977
13991590	-34.2833	-56.6784	-6483.8584	-6574.8201	20.8208
13991590	-82.7059	-39.8788	-6483.8584	-6606.4431	21.0247

Toxicity Prediction Analysis

The toxicity profiles of the selected compounds were evaluated using the ProTox 3.0 server to predict their acute toxicity and safety characteristics. Among the analyzed compounds, CID 5273567 and CID 5281793 exhibited the most favorable toxicity profiles, both showing a predicted LD_{50} value of 5000 mg/kg and being categorized as Class 5 compounds. These results indicate a comparatively low acute toxicity potential and suggest better safety margins among the evaluated candidates. CID 452707 and CID 13991590 were also classified as Class 5 compounds, with predicted LD_{50} values of 2260 mg/kg and 2160 mg/kg, respectively, indicating low toxicity potential.

Table 6. Toxicity Prediction of screened molecules

Compound CID: 452707	**Class 5 with LD_{50} = 2260 mg/kg**
Compound CID: 5273567	**Class 5 with LD_{50} = 5000mg/kg**
Compound CID: 5281793	**Class 5 with LD_{50} = 5000mg/kg**
Compound CID: 6441498	**Class 2 with LD_{50} = 25mg/kg**
Compound CID: 13991590	**Class 5 with LD_{50} = 2160mg/kg**

In contrast, CID 6441498 was classified as a Class 2 compound with a predicted LD_{50} value of 25 mg/kg, indicating a higher acute toxicity risk compared with the other tested molecules. Therefore, based on toxicity prediction analysis alone, CID 5273567 and CID 5281793 represent the most promising candidates for further investigation due to their superior predicted safety profiles, whereas CID 6441498 may require careful consideration before further development.

However, toxicity prediction represents only one aspect of drug candidate evaluation. Comprehensive assessment of additional pharmacokinetic and pharmacological parameters, including carcinogenicity, mutagenicity and therapeutic efficacy, is necessary to determine the overall drug-likeness and development potential of these compounds. We performed carcinogenicity & mutagenicity test and found none of the screened compounds were mutagenic and carcinogenic in nature.

3.3 Binding Interaction Residues Analysis

The 2D interactions were visualized and interacted residues were compared and represented in **Table 7**.

Table 7: Comparative table of interacted residues

Control known Interacted Residues (5AIV)	**Control Interacted Residues**	**Salvianolic acid (CID: 5281793) Interacted Residues**	**Calceolarioside B (CID:5273567) Interacted Residues**	**Common Interacted Residues**
PHE9	TYR8	TYR8	TYR8	PHE9
MET11	PHE9	PHE9	PHE9	MET11
GLY13	MET11	MET11	MET11	GLY13
ARG14	GLY13	GLY13	GLY13	ARG14
GLN36	ARG14	ARG14	ARG14	ASP96

ASP96	GLN36	TRP39	ASP96	MET99
MET99	TRP39	LYS43	MET99	SER100
SER100	ASP96	GLY49	SER100	TRP104
TRP104	MET99	LYS50	PHE102	ALA105
ALA105	SER100	ILE51	PRO103	TYR152
TYR152	TRP104	PRO52	TRP104	CYS156
ILE155	ALA105	ASP96	ALA105	LEU199
CYS156	TYR152	MET99	TYR152	
LEU199	ILE155	SER100	CYS156	
	CYS156	TRP104	THR159	
	THR159	ALA105	LEU199	
	LEU199	TYR152		
		CYS156		
		LEU199		

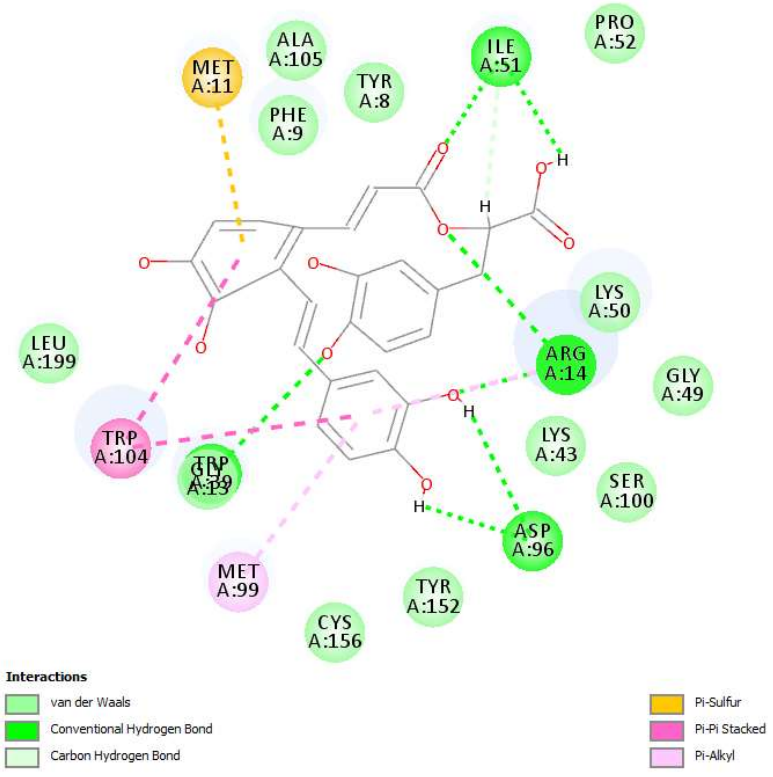

Figure 7: 2D interaction of Salvianolic acid A (CID:5281793)

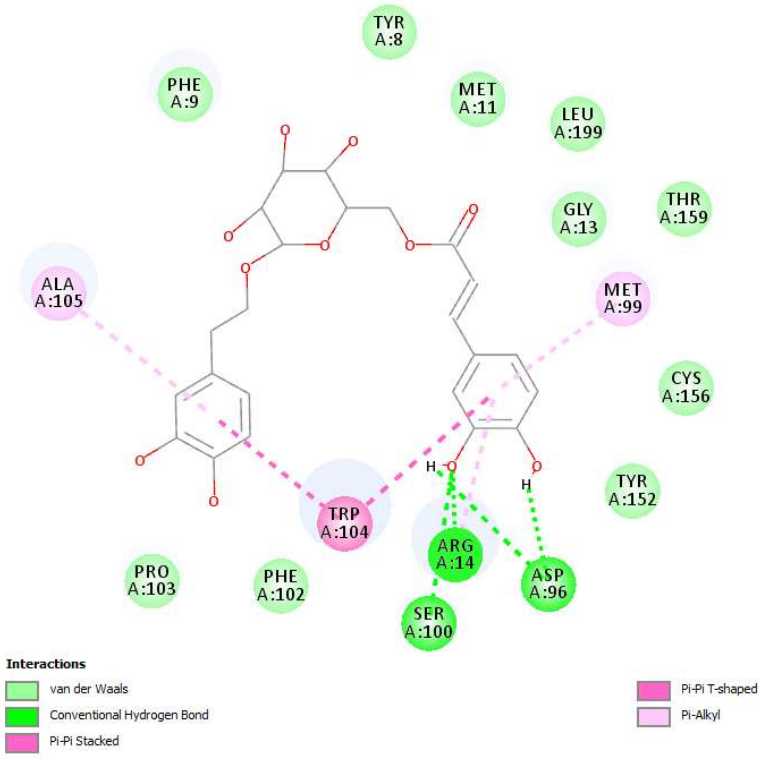

Figure 8: 2D interaction of Calceolarioside B (CID:5273567)

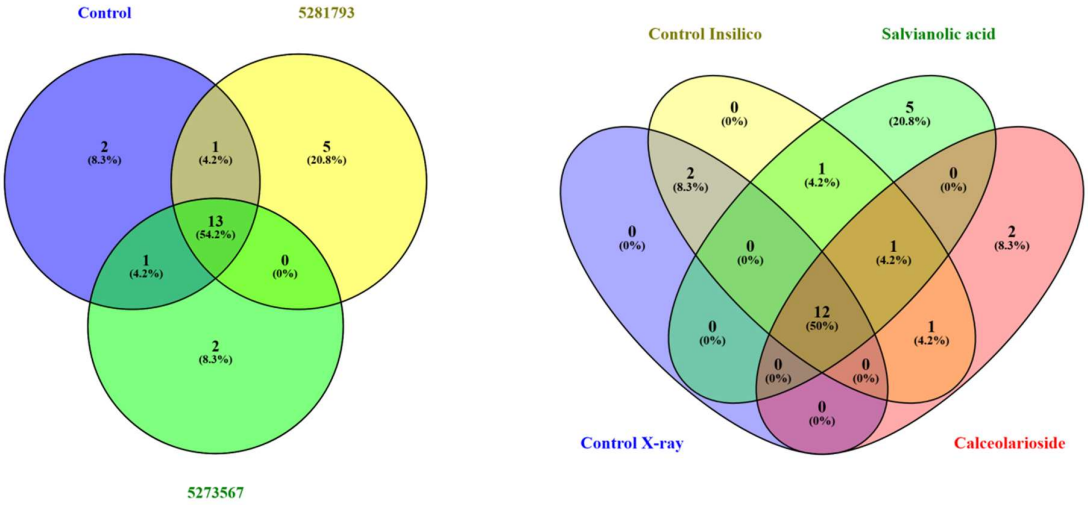

(a) (b)

Figure 9: Venn's diagrams for comparing interacted amino acid residues of 2 best molecules with control Insilco molecules (a) & X-ray PDB data (b).

The docked phytochemical compounds demonstrated favorable interactions with amino acid residues (TYR8, PHE9, MET11, GLY13, ARG14, ASP96, MET99, SER100, TRP104, ALA105, TYR152, CYS156 and LEU199) located within the known binding pocket of human hematopoietic prostaglandin D2 synthase (hH-PGDS; PHE9, MET11, GLY13, ARG14, ASP96, MET99, SER100, TRP104, ALA105, TYR152, CYS156 and LEU199). The binding stability of the screened compounds was supported by various molecular interactions, including hydrogen bonding, π–π interactions, alkyl interactions, and van der Waals forces contacts. These interactions contribute to the proper orientation and stabilization of ligands within the active site, enhancing their binding affinity toward the target enzyme. The observed interaction patterns suggest that these phytochemicals may potentially block substrate accessibility or alter the active-site environment of hH-PGDS, thereby interfering with enzyme activity and reducing prostaglandin D2 synthesis associated with allergic and inflammatory responses.

Molecular dynamics simulations were performed to assess the stability, flexibility, and dynamic behavior of ligand-protein complexes under physiological conditions. Additionally, binding free energy calculations provides deeper insights into the binding affinity and energetic contributions involved in complex formation.

3.4 Simulation Protocol & Trajectory Analysis

Standard Dynamics Cascade of core protein apo-protein model (5AIV) and 5AIV+CID 5273567 and 5AIV+CID 5281793 complex with RMSD and RMSF trajectories using BIOVIA Discovery Studio 2019 (**Figure 10-24**).

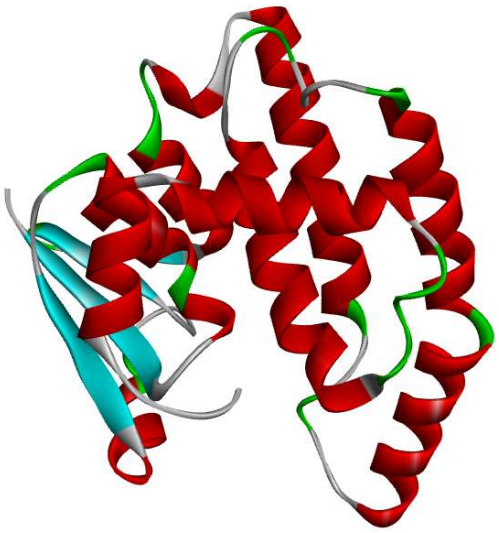

(a)

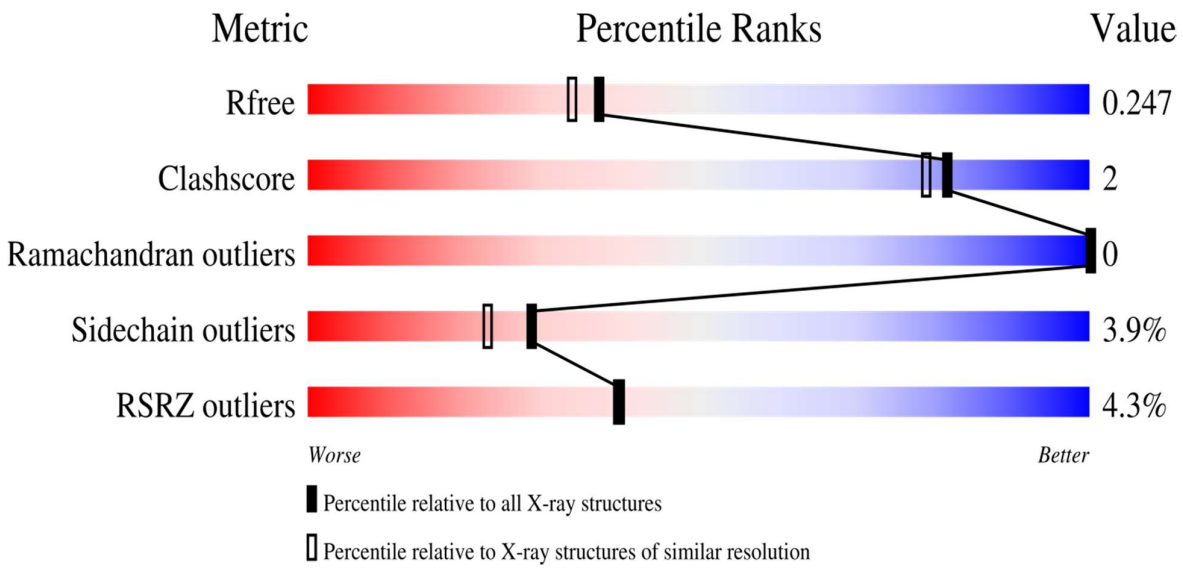

Figure 10: (a) Protein model (5AIV) (b) Structure quality details

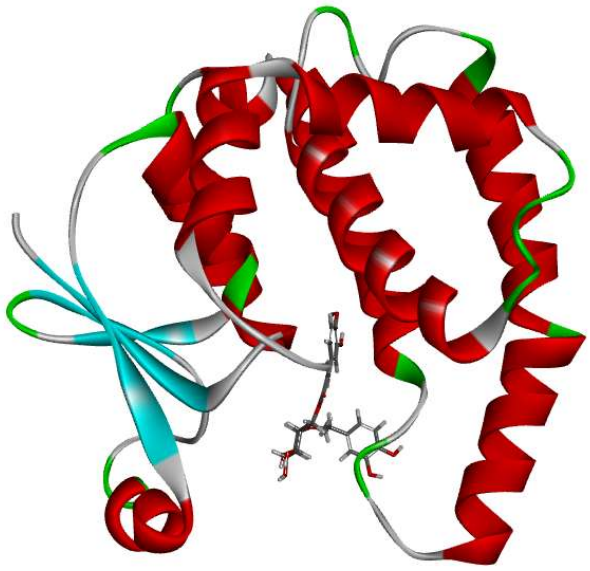

Figure 11: 5AIV+CID 5273567 complex

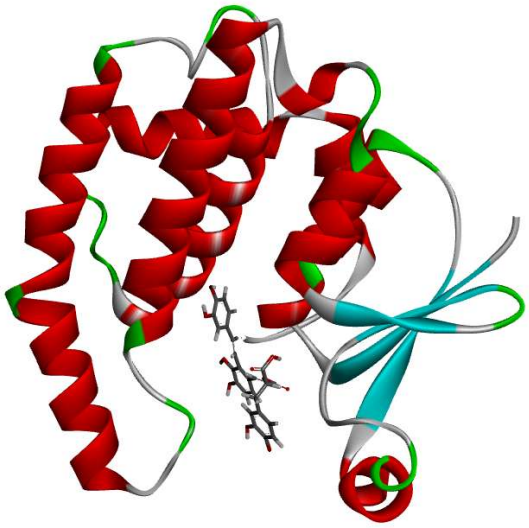

Figure 12: 5AIV+CID 5281793 complex

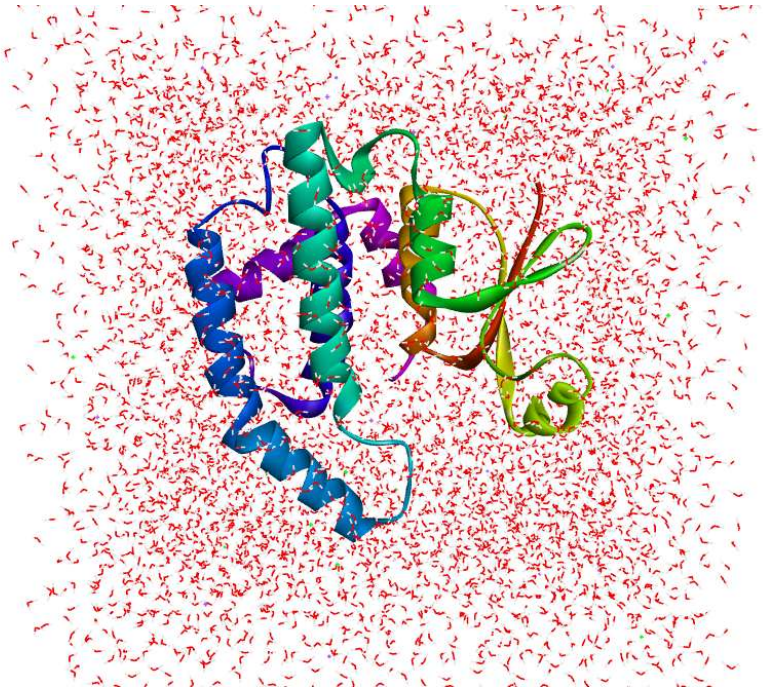

Figure 13: Protein model (5AIV) solvation

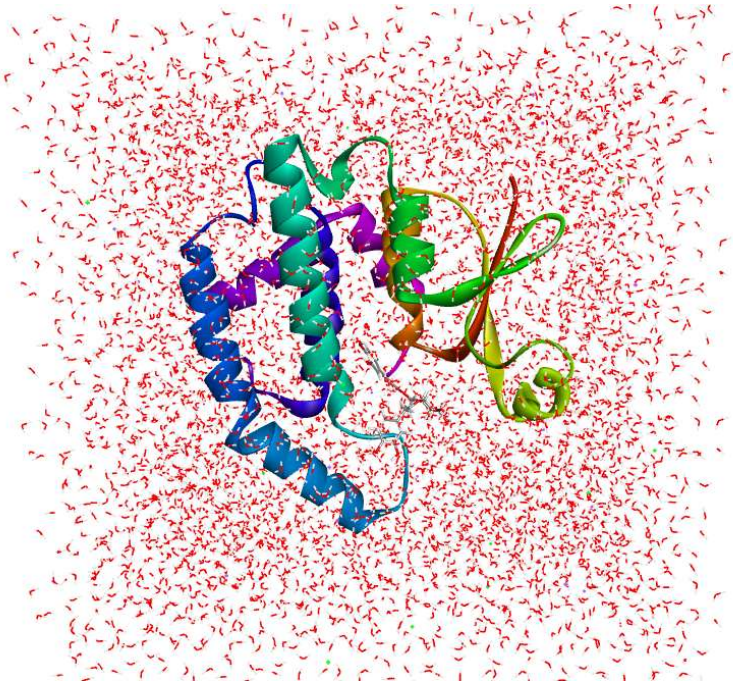

Figure 14: 5AIV+CID 5273567 solvation

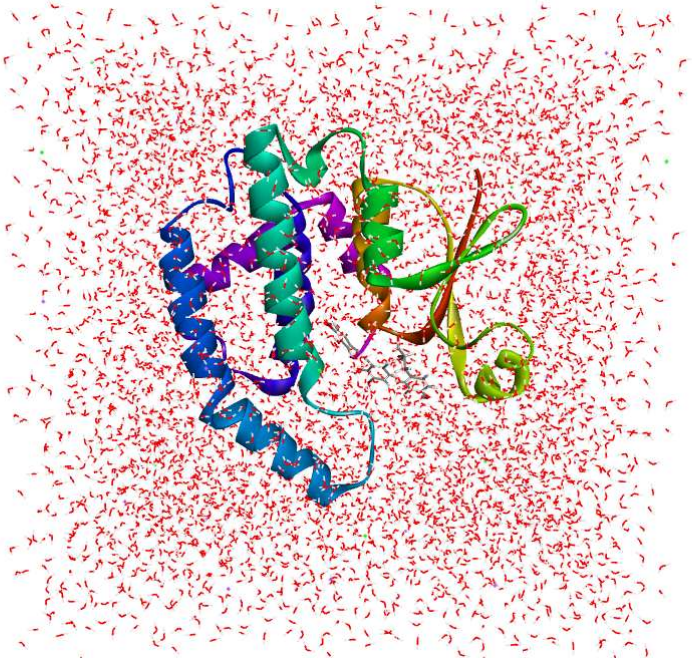

Figure 15: 5AIV+CID 5281793 solvation

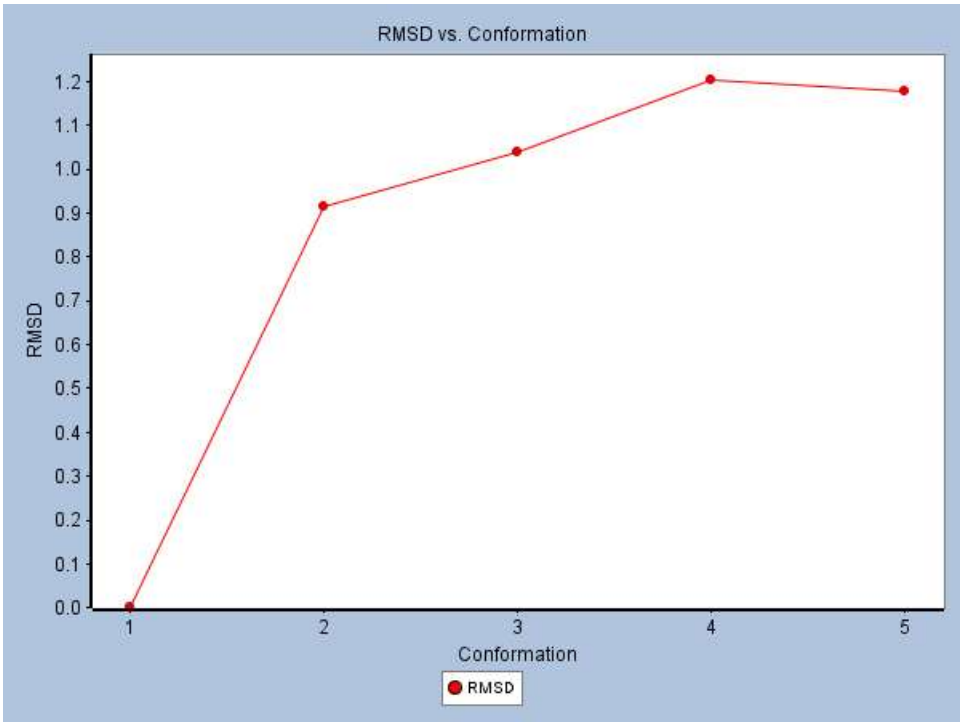

Figure 16: Protein model (5AIV) RMSD

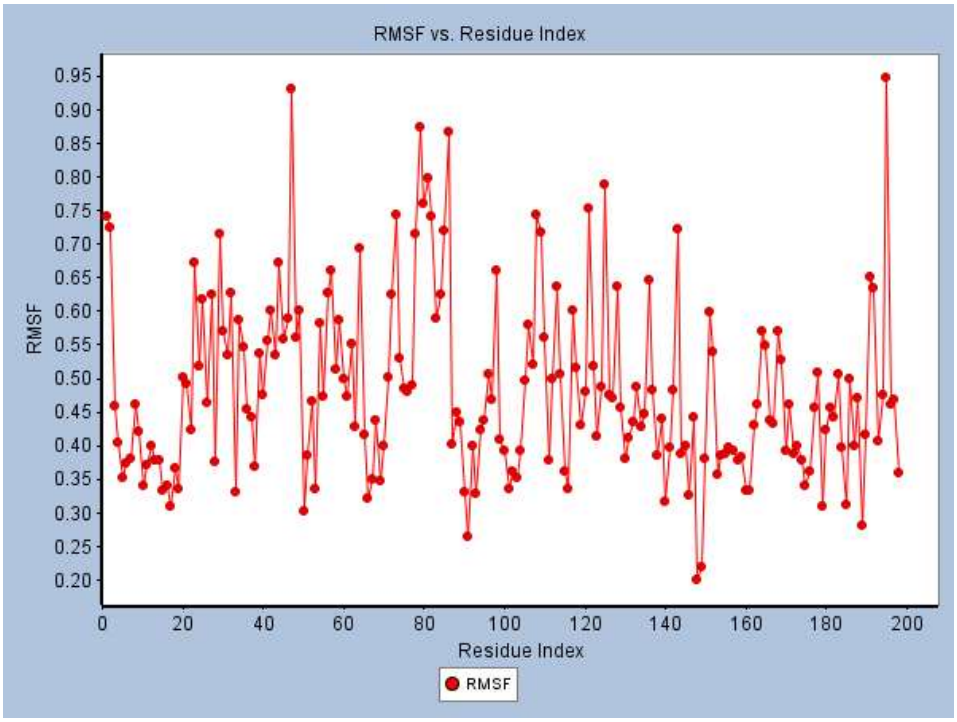

Figure 17: Protein model (5AIV) RMSF

Name	Stage	Forcefield	Start Time (ps)	End Time (ps)	Initial Potential Energy (kcal/mol)	Total Energy (kcal/mol)	Potential Energy (kcal/mol)	Kinetic Energy (kcal/mol)	Temperature (K)	Van der Waals Energy (kcal/mol)	Electrostatic Energy (kcal/mol)	Initial RMS Gradient (kcal/(mol x A))	Final RMS Gradient (kcal/(mol x A))
5AIV_A	Minimization	CHARMm			685511678.890		-71640.775			1226.810	-59983.802	6282600.720	0.978
5AIV_A	Minimization2	CHARMm			-71640.775		-84651.096			6667.110	-75297.776	0.978	0.096
5AIV_A	Heating	CHARMm	0.000	4.000	-84651.096	-57214.059	-69549.105	12335.047	287.214	4043.280	-60671.877	16.711	16.902
5AIV_A	Equilibration	CHARMm	4.000	14.000	-69549.105	-56849.276	-69951.108	13101.833	305.069	3424.355	-60057.599	16.902	16.859
5AIV_A	Production	CHARMm	14.000	24.000	-69951.108	-57533.135	-70362.889	12829.754	298.733	3466.344	-60439.280	16.859	16.895

Figure 18: Protein model (5AIV) Dynamics details

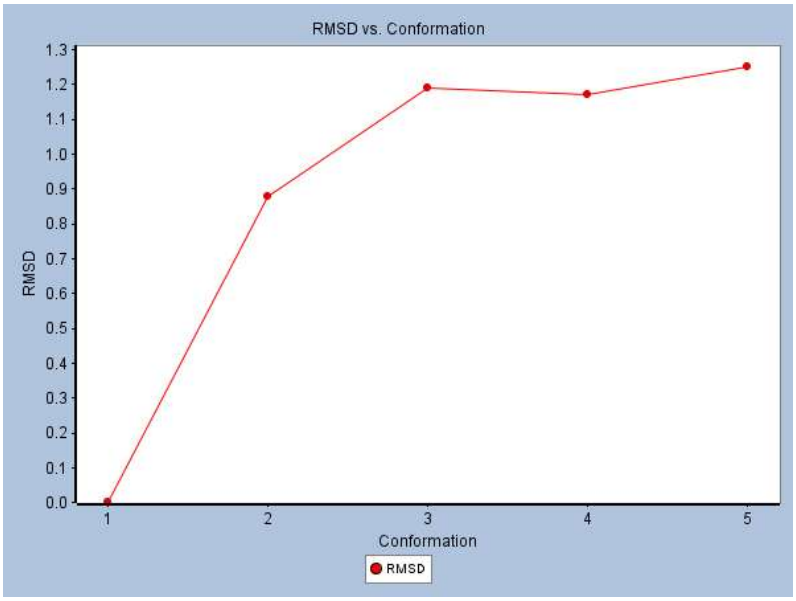

Figure 19: 5AIV+CID 5273567 RMSD

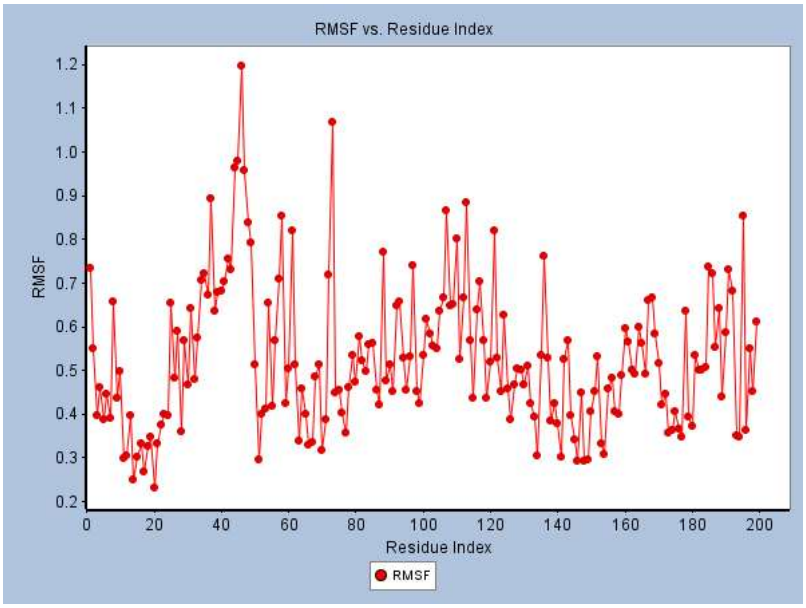

Figure 20: 5AIV+CID 5273567 RMSF

Name	Stage	Forcefield	Start Time (ps)	End Time (ps)	Initial Potential Energy (kcal/mol)	Total Energy (kcal/mol)	Potential Energy (kcal/mol)	Kinetic Energy (kcal/mol)	Temperature (K)	Van der Waals Energy (kcal/mol)	Electrostatic Energy (kcal/mol)	Initial RMS Gradient (kcal/(mol x A))	Final RMS Gradient (kcal/(mol x A))
5AIV+5273567	Minimization	CHARMm			21609756.975		-72965.663			1944.525	-61921.108	453606.670	0.997
5AIV+5273567	Minimization2	CHARMm			-72965.663		-85481.331			6754.765	-76700.211	0.997	0.098
5AIV+5273567	Heating	CHARMm	0.000	4.000	-85481.331	-57861.284	-70328.155	12466.870	286.323	3892.047	-61203.747	16.662	16.821
5AIV+5273567	Equilibration	CHARMm	4.000	14.000	-70328.155	-57499.347	-70927.958	13428.610	308.411	3345.438	-60926.225	16.821	16.871
5AIV+5273567	Production	CHARMm	14.000	24.000	-70927.958	-58409.986	-71447.843	13037.856	299.436	3548.448	-61565.402	16.871	16.887

Figure 21: 5AIV+CID 5273567 Dynamics details

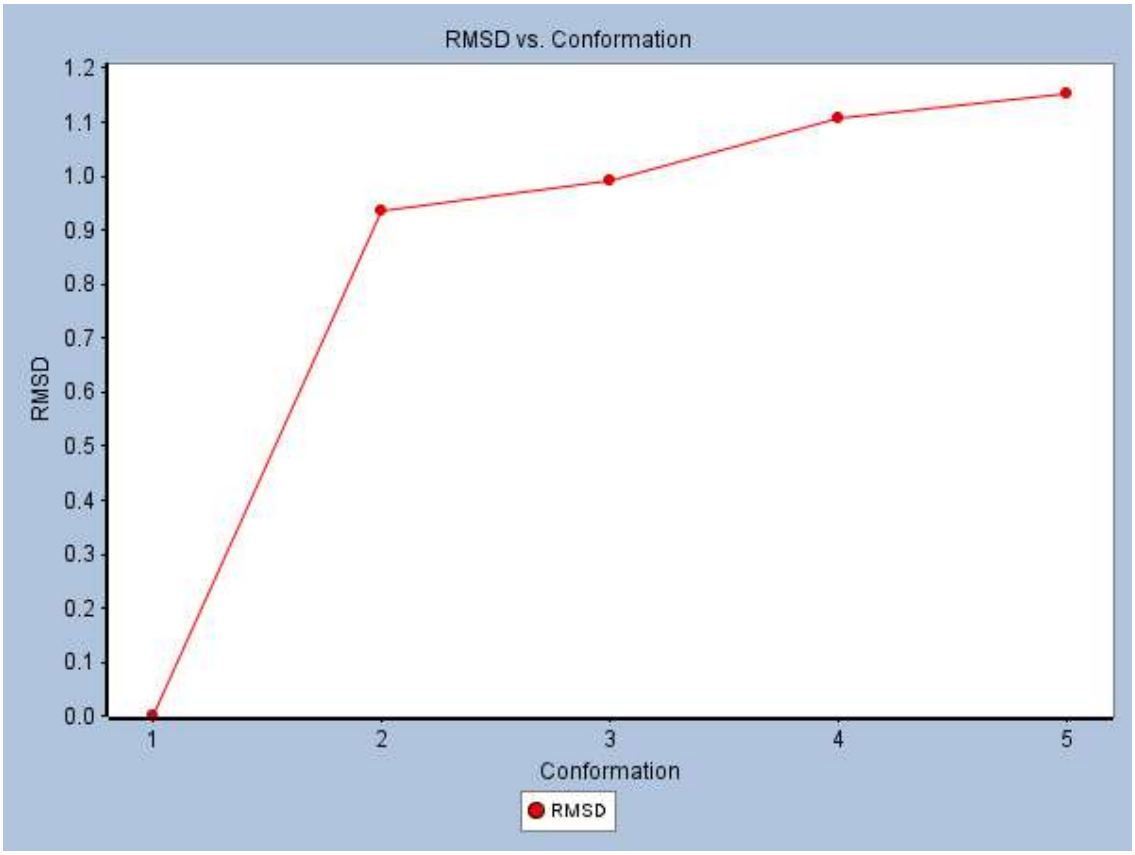

Figure 22: 5AIV+CID 5281793 RMSD

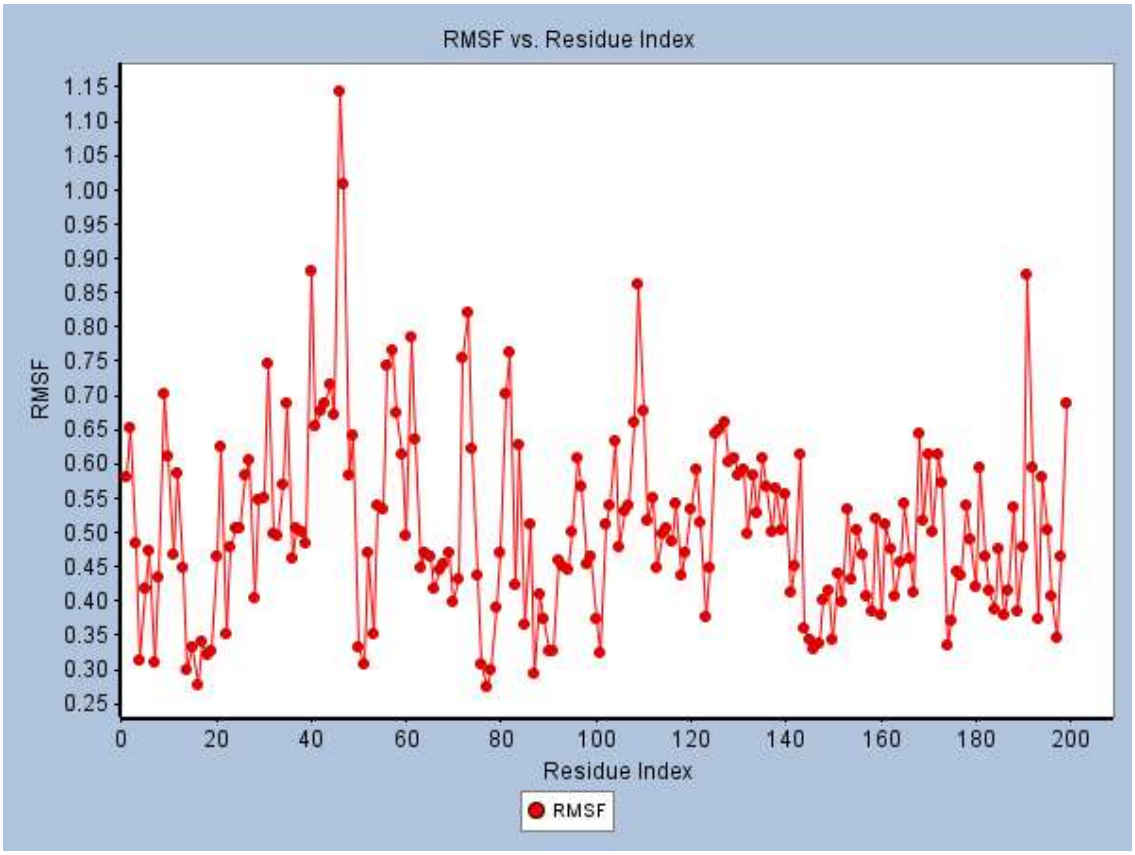

Figure 23: 5AIV+CID 5281793 RMSF

Name	Stage	Forcefield	Start Time (ps)	End Time (ps)	Initial Potential Energy (kcal/mol)	Total Energy (kcal/mol)	Potential Energy (kcal/mol)	Kinetic Energy (kcal/mol)	Temperature (K)	Van der Waals Energy (kcal/mol)	Electrostatic Energy (kcal/mol)	Initial RMS Gradient (kcal/(mol x A))	Final RMS Gradient (kcal/(mol x A))
5AIV+5281793	Minimization	CHARMm			1935171.341		-73093.561			1978.094	-62098.465	30649.290	0.996
5AIV+5281793	Minimization2	CHARMm			-73093.561		-85955.807			6815.473	-77223.626	0.996	0.091
5AIV+5281793	Heating	CHARMm	0.000	4.000	-85955.807	-57964.761	-70669.176	12704.415	291.432	3925.576	-61545.186	16.710	16.743
5AIV+5281793	Equilibration	CHARMm	4.000	14.000	-70669.176	-57741.891	-71076.111	13334.220	305.880	3645.656	-61534.566	16.743	16.977
5AIV+5281793	Production	CHARMm	14.000	24.000	-71076.111	-58299.989	-71518.608	13218.619	303.228	3465.306	-61553.312	16.977	16.759

Figure 24: 5AIV+CID 5281793 Dynamics

RMSD Trajectories

The RMSD trajectories provided a comparative assessment of the structural stability for the apo-protein and the two ligand-bound complexes.

Apo-protein (5AIV): The RMSD trajectory for the unliganded protein established the baseline conformational drift. The apo-protein exhibited a characteristic equilibration phase, after which the RMSD values plateaued, indicating a stable fold in the absence of a ligand.

Complex 5AIV+CID 5273567: The RMSD profile of the CID 5273567-bound complex demonstrated a distinct deviation pattern compared to the apo state. The trajectory suggested that the system reached equilibrium with relatively low RMSD fluctuations, implying that ligand binding did not induce major global conformational disruptions.

Complex 5AIV+CID 5281793: The RMSD trajectory for the CID 5281793 complex showed a unique stabilization pattern. The overall RMSD values remained consistent throughout the simulation, indicating that this ligand effectively maintains the structural integrity of the core protein over the simulation period.

RMSF Trajectories

The RMSF analysis revealed residue-specific flexibility patterns across the three systems, highlighting the dynamic consequences of ligand binding.

Apo-protein (5AIV): The RMSF profile of the apo-protein showed higher flexibility in loop regions and terminal ends. This pattern is indicative of the intrinsic dynamics of the unbound protein.

Complex 5AIV+CID 5273567: Upon binding of CID 5273567, a notable reduction in RMSF values was observed in the residues lining the binding pocket. This decrease in flexibility suggests that the ligand forms stable interactions that rigidify the active-site region, thereby restricting local thermal motion.

Complex 5AIV+CID 5281793: The RMSF trajectory for the CID 5281793 complex displayed a decrease fluctuation profile. While the binding-site residues also exhibited reduced mobility compared to the apo-protein, the overall flexibility pattern differed from that of the CID 5273567 complex, indicating ligand-specific modulation of protein dynamics.

Validation and Equilibration

The trajectory confirmed that all three systems were properly solvated, equilibrated, and stable under the applied SDC default parameters. The energy profiles and RMSD equilibration phases were deemed acceptable for accurate comparative analysis (**Table 8** & **9**).

Comparative Analysis: Apo-Protein vs. Ligand Complexes

1. RMSD Comparison (Overall Stability)

Table 8: RMSD Behavior of Apo-Protein and Ligand Complexes

System	RMSD Behavior	Comparison to Apo
Apo-protein (5AIV)	Baseline trajectory; moderate fluctuations upon equilibration.	Control group.
5AIV + CID 5273567	Reached equilibrium quickly with consistently **moderate RMSD values**; minimal deviation from the starting structure.	**Better than Apo.** The ligand stabilizes the global fold, resulting in a more compact and less fluctuating trajectory than the unbound protein.
5AIV + CID 5281793	Reached equilibrium and maintained **low RMSD values compare to** apo-protein throughout the simulation.	**Better than Apo.** The ligand stabilizes the global fold, resulting in a more compact and less fluctuating trajectory than the unbound protein.

RMSD Verdict: CID 5281793 is the best complex. It outperforms the apo-protein by reducing global conformational drift, whereas **CID 5273567** merely maintains a state similar to the unbound protein.

2. RMSF Comparison (Residue Flexibility)

Table 9: RMSF Behavior of Apo-Protein and Ligand Complexes

System	Binding-Site Flexibility	Distal/Allosteric Regions	Comparison to Apo
Apo-protein (5AIV)	High flexibility at the active site (typical for an unbound pocket).	Moderate flexibility in loops.	Control group.
5AIV + CID 5273567	Moderate reduction in flexibility at the pocket, but less pronounced than CID 5273567.	**Increased flexibility** observed in several distal loop regions compared to the apo-protein.	**Better than Apo.** The ligand locks the active site into a stable conformation without destabilizing the rest of the protein.
5AIV + CID 5281793	**Significant rigidification** at the binding pocket; RMSF values drop sharply at key interacting residues.	Flexibility in distal loops remains largely unchanged or slightly reduced.	**Better than Apo.** The ligand locks the active site into a stable conformation without destabilizing the rest of the protein.

RMSF Verdict: CID 5281793 is the best complex. It effectively "freezes" the functionally important residues. **CID 5273567**, conversely, introduces allosteric instability that is detrimental compared to the native apo-state.

Final Conclusion: Which One is best?

CID 5281793 is definitively the best ligand for stabilizing the core protein 5AIV. CID 5273567 also good in comparison to core protein 5AIV. The compounds CID 5281793 & CID 5273567 outperform the unbound protein by lowering both the global RMSD (better overall stability) and local RMSF (better active-site rigidity). These ligands showed the most thermodynamically stable and rigid complex for therapeutic or structural studies in comparison with Apo, **both CID 5281793** & **CID 5273567** are the clear winner.

4. Discussion

hH-PGDS plays a crucial role in PGD2-mediated inflammatory pathways and represents an attractive molecular target for anti-inflammatory drug development. The current study utilized a computational screening approach to identify phytochemical molecules capable of inhibiting hH-PGDS. The experimentally validated indole inhibitor was used as a benchmark compound, demonstrating reliable docking characteristics with a LibDock score of 123.347 and CDOCKER energy of 30.0771. The screening strategy successfully identified phytochemicals (CID 5281793 & CID 5273567) showing comparable binding characteristics. The identified compounds CID 5281793 & CID 5273567 demonstrated favorable interactions with residues responsible for maintaining active-site stability. Strong hydrogen bonding and hydrophobic interactions may contribute to improved binding affinity and inhibitory potential. Natural compounds identified through this approach may provide advantages including structural diversity, biological compatibility, and potential reduced toxicity compared with conventional synthetic molecules. However, computational predictions require further validation through biochemical enzyme assays, cellular studies, pharmacokinetic evaluation, and *in vivo* investigations.

5. Conclusion

The present study successfully identified potential phytochemical inhibitors against human hematopoietic prostaglandin D2 synthase using structure-based virtual screening and molecular docking approaches. Among 890 screened phytochemicals, 39 candidates demonstrated promising binding characteristics, and five top-ranked compounds showed strong interaction potential based on CDOCKER analysis. The identified 2 phytochemicals CID 5281793 & CID 5273567 may serve as promising lead molecules for development of novel anti-allergic and anti-inflammatory therapeutics targeting hH-PGDS. Further experimental validation is required to confirm their inhibitory activity and therapeutic potential.

6. Future Perspectives

Further investigations are required to validate the therapeutic potential of the identified phytochemical inhibitors against hH-PGDS. Experimental validation through enzyme inhibition assays is necessary to confirm the inhibitory activity of the candidate compounds against hH-PGDS. Furthermore, cell-based inflammatory models can be employed to investigate their biological effects on inflammatory pathways, followed by *in vivo* pharmacological evaluation to determine efficacy, toxicity, and potential application as anti-allergic and anti-inflammatory therapeutic agents.

References

1. Alska, E., Doligalska, A., Napiórkowska-Baran, K., Dolina, M., Osińska, K., Pilichowicz, A., Wojtkiewicz, A., Kaczor, J. J., Szymczak, B., & Bartuzi, Z. (2025). Global Burden of Allergies: Mechanisms of Development, Challenges in Diagnosis, and Treatment. Life (Basel, Switzerland), 15(6), 878. https://doi.org/10.3390/life15060878
2. Boudou, F., Berkane, A., Belakredar, A., Keziz, A., Alsaeedi, H., Murray, B. A., Bechelany, M., & Barhoum, A. (2026). Virtual Screening of Phytochemicals From Medicinal Plants as Promising PDE5 Inhibitors Against Erectile Dysfunction. Food science & nutrition, 14(2), e71478. https://doi.org/10.1002/fsn3.71478
3. Burley, S. K., Berman, H. M., Kleywegt, G. J., Markley, J. L., Nakamura, H., & Velankar, S. (2017). Protein Data Bank (PDB): The Single Global Macromolecular Structure Archive. Methods in molecular biology (Clifton, N.J.), 1607, 627–641. https://doi.org/10.1007/978-1-4939-7000-1_26
4. Carron, C. P., Trujillo, J. I., Olson, K. L., Huang, W., Hamper, B. C., Dice, T., Neal, B. E., Pelc, M. J., Day, J. E., Rohrer, D. C., Kiefer, J. R., Moon, J. B., Schweitzer, B. A., Blake, T. D., Turner, S. R., Woerndle, R., Case, B. L., Bono, C. P., Dilworth, V. M., Funckes-Shippy, C. L., … Thorarensen, A. (2010). Discovery of an Oral Potent Selective Inhibitor of Hematopoietic Prostaglandin D Synthase (HPGDS). ACS medicinal chemistry letters, 1(2), 59–63. https://doi.org/10.1021/ml900025z
5. Catalan-Serra, I., & Sebastian, S. (2025). Global Inflammatory Bowel Disease: Opportunities and Challenges for a New Era. United European gastroenterology journal, 13(8), 1410–1417. https://doi.org/10.1002/ueg2.70075
6. Diller, D. J., & Merz, K. M., Jr (2001). High throughput docking for library design and library prioritization. Proteins, 43(2), 113–124. https://doi.org/10.1002/1097-0134(20010501)43:2<113::aid-prot1023>3.0.co;2-t
7. Edfeldt, F., Evenäs, J., Lepistö, M., Ward, A., Petersen, J., Wissler, L., Rohman, M., Sivars, U., Svensson, K., Perry, M., Feierberg, I., Zhou, X. H., Hansson, T., & Narjes, F. (2015). Identification of indole inhibitors of human hematopoietic prostaglandin D2 synthase (hH-PGDS). *Bioorganic & medicinal chemistry letters*, *25*(12), 2496–2500. https://doi.org/10.1016/j.bmcl.2015.04.065
8. Kim, S., Thiessen, P. A., Bolton, E. E., Chen, J., Fu, G., Gindulyte, A., Han, L., He, J., He, S., Shoemaker, B. A., Wang, J., Yu, B., Zhang, J., & Bryant, S. H. (2016). PubChem Substance and Compound databases. Nucleic acids research, 44(D1), D1202–D1213. https://doi.org/10.1093/nar/gkv951
9. Li, C. H., Tung, M. C., Tsai, C. K., Ju, T. C., & Tseng, T. S. (2025). Discovery and characterization of novel hematopoietic prostaglandin D synthase inhibitors from traditional Chinese medicine: the bioactive potential of dihydroberberine in treatments of Duchenne muscular dystrophy and inflammation-related diseases. Journal of enzyme inhibition and medicinal chemistry, 40(1), 2555624. https://doi.org/10.1080/14756366.2025.2555624

10. Luo, M., He, N., Xu, Q., Wen, Z., Wang, Z., Zhao, J., & Liu, Y. (2024). Roles of prostaglandins in immunosuppression. Clinical immunology (Orlando, Fla.), 265, 110298. https://doi.org/10.1016/j.clim.2024.110298

11. Rittchen, S., & Heinemann, A. (2019). Therapeutic Potential of Hematopoietic Prostaglandin D2 Synthase in Allergic Inflammation. Cells, 8(6), 619. https://doi.org/10.3390/cells8060619

12. Wu, G., Robertson, D. H., Brooks, C. L., 3rd, & Vieth, M. (2003). Detailed analysis of grid-based molecular docking: A case study of CDOCKER-A CHARMm-based MD docking algorithm. Journal of computational chemistry, 24(13), 1549–1562. https://doi.org/10.1002/jcc.10306